

Searching for Charged Higgs Bosons via $e^+e^- \rightarrow H^+H^- \rightarrow c\bar{b}\bar{c}b$ at Linear Colliders

Wei-Shu Hou^a Rishabh Jain^a Tanmoy Modak^b

^a*Department of Physics, National Taiwan University, Taipei 10617, Taiwan*

^b*Institut für Theoretische Physik, Universität Heidelberg, 69120 Heidelberg, Germany*

E-mail: wshou@phys.ntu.edu.tw, rishabhjain@hep1.phys.ntu.edu.tw,
tanmoy@thphys.uni-heidelberg.de

ABSTRACT: We study a search for the charged Higgs boson via $e^+e^- \rightarrow H^+H^- \rightarrow c\bar{b}\bar{c}b$ at the 500 GeV ILC. In a general two Higgs doublet model without Z_2 symmetry, extra Yukawa couplings ρ_{tt} and ρ_{tc} can drive baryogenesis, but searches at the HL-LHC may still go empty-handed if the couplings are relatively weak. Taking $m_{H^+} \simeq m_H \simeq m_A \simeq 200$ GeV, with $\rho_{tt}, \rho_{tc} \sim 0.1$ and no $h(125)$ - H mixing, $H^+ \rightarrow c\bar{b}$ decay is dominant, and the $c\bar{b}\bar{c}b$ final state is likely overwhelmed by QCD background at the LHC. We show that the electroweak production of H^+H^- at the ILC is discoverable with integrated luminosity of 1 ab^{-1} . Furthermore, we show that m_{H^+} can be extracted by requiring the two pairs of b and light jets be roughly equal in mass, without assuming the mass value. Thus, ILC can probe low mass Higgs bosons in multijet final states to complement HL-LHC in the future.

KEYWORDS: Beyond Standard Model, Higgs Physics, Flavor violation

ARXIV EPRINT: [2111.06523](https://arxiv.org/abs/2111.06523)

Contents

1	Introduction	1
2	Framework and Signal Process	3
3	Signal and background processes	4
4	Prospects for Discovery and Mass Extraction	7
5	Discussion and Conclusion	10

1 Introduction

Many extensions of the Standard Model (SM) predict the existence of extra Higgs bosons, for example, to provide additional CP violation required for baryogenesis, to account for matter dominance of the Universe [1, 2]. In this report we consider the general two Higgs doublet model (g2HDM) without Z_2 symmetry, where after electroweak symmetry breaking (EWSB) one has 5 Higgs bosons: two CP -even neutral scalars h, H , one CP -odd scalar A , and charged scalars H^\pm . Without a Z_2 symmetry, one has an extra set of Yukawa couplings for each type of charged fermion f . In general, ρ^f cannot be diagonalized simultaneously with the mass matrix m^f , leading to flavor changing neutral couplings (FCNC). As these are usually considered as dangerous, Natural Flavor Conservation was proposed [3] to kill the extra Yukawa couplings, hence avoid FCNCs altogether. We advocate, however, that one should leave the final say on the matter to the experiments.

It was shown [1, 4] that extra top-Yukawa couplings ρ_{tt} and ρ_{tc} can drive electroweak baryogenesis (EWBG). Following this motivation, it was pointed out that $cg \rightarrow tH/tA \rightarrow tt\bar{c}, t\bar{t}$ [5] can provide same-sign top and triple-top signatures at the LHC. However, $\mathcal{O}(1)$ values of ρ_{tc} is constrained by [6, 7] from CRW, a Control Region for $t\bar{t}W$ background in the 4-top study by CMS [8]. On the other hand, ρ_{tt} is constrained by $b \rightarrow s\gamma$ and $B-\bar{B}$ mixing [9]. All these limits are modulated by the unknown scalar masses, except the already observed $h(125)$ [10, 11]. With rich dynamics and sub-TeV extra Higgs bosons [12], the g2HDM can provide very rich signatures at the LHC [13] and impact on flavor physics [14].

ATLAS and CMS have performed many searches for extra scalars in different channels, such as $H/A \rightarrow \tau\tau$ [15, 16], $H \rightarrow \tau\mu$ [17], $H/A \rightarrow b\bar{b}$ [18, 19], $H, A \rightarrow t\bar{t}$ [20, 21], $H^+ \rightarrow t\bar{b}$ [22, 23], $H^+ \rightarrow cs$ [24, 25], $H^+ \rightarrow \tau\nu$ [26, 27], and over broad mass ranges. But a scalar of mass around 200 GeV decaying into jets is relatively challenging for the LHC due to high QCD backgrounds. Furthermore, cross sections become challenging at the LHC if the extra top Yukawa couplings are considerably below $\mathcal{O}(1)$ [13]. For the special case of sizable ρ_{tc} but all other extra Yukawa couplings negligible in strength, the cancellation between

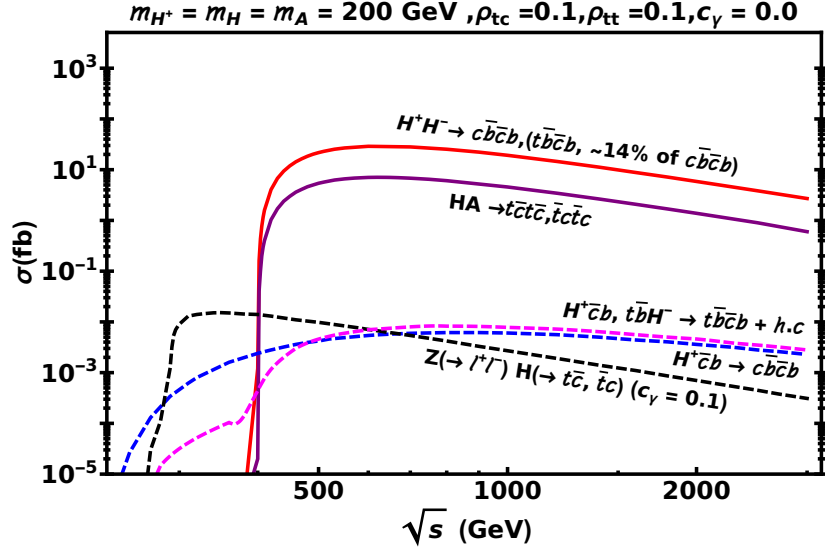


Figure 1. Cross section vs \sqrt{s} for $e^+e^- \rightarrow H^+H^- \rightarrow \bar{c}\bar{b}cb$ (red, solid), $HA \rightarrow t\bar{c}t\bar{c}, \bar{t}c\bar{t}c$ (purple solid), $Z(\rightarrow \ell\ell)H(\rightarrow \bar{t}\bar{c}, \bar{t}c)$ (black, dashed, with $c_\gamma = 0.1$), $H^+\bar{c}b \rightarrow \bar{c}\bar{b}cb$ (blue, dashed), and $H^+\bar{c}b, \bar{t}bH^- \rightarrow \bar{t}\bar{b}\bar{c}b + \text{h.c.}$ (magenta, dashed). Note here that the c_γ is nonvanishing only for $Z(\rightarrow \ell\ell)H(\rightarrow \bar{t}\bar{c}, \bar{t}c)$ process but set to zero for all other curves and throughout the manuscript.

H and A for $cg \rightarrow tH/tA \rightarrow tt\bar{c}$ [5, 13] again makes the extra scalars unobservable at the LHC. In this report, we propose that if a light H^+ decaying hadronically remains elusive at the High Luminosity LHC (HL-LHC), a linear e^+e^- collider with sub-TeV energies would be able to probe m_{H^+} at $\mathcal{O}(200)$ GeV through $e^+e^- \rightarrow H^+H^- \rightarrow \bar{c}\bar{b}cb$. Similar processes have been proposed previously for $m_{H^+} \lesssim M_Z$ [28–30].

We take $\rho_{tc} = \rho_{tt} = 0.1$ to evade HL-LHC search [13]. We assume degenerate $m_{H^+} = m_H = m_A = 200$ GeV, and take the alignment limit of vanishing h - H mixing ($c_\gamma \equiv \cos \gamma \rightarrow 0$) to reduce the number of parameters. Our focus will be the electroweak production process

$$e^+e^- \rightarrow \gamma^*/Z^* \rightarrow H^+H^- \rightarrow \bar{c}\bar{b}cb. \quad (1.1)$$

Then $\rho_{tc} = \rho_{tt} \sim 0.1$ means $\bar{t}\bar{b}\bar{c}b$ (plus conjugate) cross section is at 14% of $\bar{c}\bar{b}cb$, as illustrated in Fig. 1, and provides a probe of ρ_{tt} . But for $|\rho_{tt}| \ll |\rho_{tc}|$, the process of Eq. (1.1) becomes independent of ρ_{tc} , provided it is the single dominant coupling. However, the 4-jet final state may appear worrisome for mass extraction, hence interpretation itself of the origin of these events.

As far as interpretation is concerned, it was suggested [31] long ago that the companion process

$$e^+e^- \rightarrow Z^* \rightarrow HA \rightarrow t\bar{c}t\bar{c}, \bar{t}c\bar{t}c, \quad (1.2)$$

can provide same-sign top plus two jet signature, with cross section (see Fig. 1) $\sim 1/3$ of $\bar{c}\bar{b}cb$ from H^+H^- production, which can support the g2HDM interpretation. But it would not help mass extraction, as same-sign top requires both tops to decay semi-leptonically.

For sake of helping the extraction of exotic Higgs mass, by analogy with Zh production, where $Z \rightarrow \ell\ell$ would tag the recoil mass, the process $e^+e^- \rightarrow Z^* \rightarrow ZH$ comes to mind. Unfortunately, this process is suppressed by c_γ^2 (see Fig. 1 for the case of $c_\gamma = 0.1$), and statistics would likely be insufficient.

As a final attempt, one has associated production of single H^+ , i.e. $e^+e^- \rightarrow Z^* \rightarrow H^+\bar{c}b \rightarrow \bar{c}\bar{c}b, \bar{t}\bar{t}b (+\text{h.c.})$ and $e^+e^- \rightarrow Z^* \rightarrow \bar{t}bH^- \rightarrow \bar{t}\bar{c}b + \text{h.c.}$, where the latter has a higher threshold. The cross sections are also given in Fig. 1, which turn out tiny because of the three-body nature and destructive interference between Zbb and Zcc diagrams. Being only a small fraction of the main process, Eq. (1.1), these can be safely ignored.

Although not intuitive at first sight, it turns out the 4-jet process of Eq. (1.1) does allow one to extract m_{H^+} . With two jets b -tagged and the c -jets untagged (achievable at ILC), one has two possible bj pairings. By demanding the two bj pairs to be close in mass, *without* specifying the mass, one not only rejects background effectively, the underlying two-body production kinematics allow the extraction of m_{H^+} , as we will show.

This report is organized as follows. We first give the framework of our study in Sec. II. We describe our signal from Eq. (1.1) and all background processes in Sec. III, and state our event selection criteria and analysis strategy. In Sec. IV, we discuss the discovery potential, method of mass extraction, and the mass window cut. After some discussions, we conclude in Sec. V.

2 Framework and Signal Process

For CP conserving Higgs sector, one can write the Higgs potential of g2HDM the Higgs basis as [12, 32]

$$V(\Phi, \Phi') = \mu_{11}^2|\Phi|^2 + \mu_{22}^2|\Phi'|^2 - (\mu_{12}^2\Phi^\dagger\Phi' + \text{h.c.}) + \frac{1}{2}\eta_1|\Phi|^4 + \frac{1}{2}\eta_2|\Phi'|^4 + \eta_3|\Phi|^2|\Phi'|^2 + \eta_4|\Phi^\dagger\Phi'|^2 + \left[\frac{1}{2}\eta_5(\Phi^\dagger\Phi')^2 + (\eta_6|\Phi|^2 + \eta_7|\Phi'|^2)\Phi^\dagger\Phi' + \text{h.c.} \right], \quad (2.1)$$

where EWSB arises from Φ while $\langle\Phi'\rangle = 0$ (hence $\mu_{22}^2 > 0$). In Eq. (2.1), η_i s are the quartic couplings and taken as real, as we assume the Higgs potential is CP -invariant. After EWSB, one can find [12] from Eq. (2.1) the mass eigenstates h, H, A and H^+ , as well as h - H mixing, where we define the mixing angle as γ .

The Yukawa couplings of the Higgs bosons to fermions are given as [32, 33],

$$-\frac{1}{\sqrt{2}} \sum_{f=u,d} \bar{f}_i \left[(\lambda_i^f \delta_{ij} c_\gamma - \rho_{ij}^f s_\gamma) H - i \text{sgn}(\mathcal{Q}_f) \rho_{ij}^f A \right] R f_j - \bar{u}_i [(V\rho^d)_{ij} R - (\rho^{u\dagger} V)_{ij} L] d_j H^+ + \text{h.c.}, \quad (2.2)$$

where i, j are summed over, $\lambda_i^f = \sqrt{2} m_i^f / v$ is the Yukawa coupling in SM, and $c_\gamma (s_\gamma) \equiv \cos \gamma (\sin \gamma)$. From Eq. (2.2) one finds that $\bar{c}bH^+$ and $\bar{t}bH^+$ couple as $\rho_{tc}V_{tb}$ and $\rho_{tc}V_{tb}$, i.e. *both* with CKM factor V_{tb} , where we have dropped CKM-suppressed terms. This may seem counterintuitive from the perspective of say 2HDM II [34], the popular 2HDM with Z_2 symmetry that automatically arises with supersymmetry, where one expects the $\bar{c}bH^+$

coupling to be suppressed by V_{cb} . It was through these couplings that $cg \rightarrow bH^+ \rightarrow bt\bar{b}$ was proposed [35] as a search mode for H^+ production, and traces back to similar arguments [36] for the V_{tb}/V_{ub} enhancement of the ρ_{tu} coupling in $B^+ \rightarrow \mu^+\nu$ decay.

Experimental searches suggest that $h(125)$ closely resembles the Higgs boson of SM, i.e. approximate alignment [37, 38]. This does not [12] necessarily imply that the sole mixing parameter, η_6 , has to be small. However, as we anticipate the case of low mass and near-degeneracy (in part to reduce the number of parameters),

$$m_{H^+} \simeq m_H \simeq m_A \simeq 200 \text{ GeV}, \quad (2.3)$$

to evade HL-LHC by decay to jets, alignment needs [12] η_6 to be small. We take $c_\gamma = 0$ again for simplicity, which can be easily put back into experimental analysis.

We can now see the reason of choosing Eq. (2.3), together with $\rho_{tc} \sim \rho_{tt} \sim 0.1$, as possibly evading HL-LHC scrutiny. The $cg \rightarrow tH/tA \rightarrow tt\bar{c}$ would suffer cancellation [5, 13] from the degeneracy while suppressed by $|\rho_{tc}|^2 \sim 0.01$; the $cg \rightarrow bH^+ \rightarrow bc\bar{b}$ process would dominate over $bt\bar{b}$, as $H^+ \rightarrow t\bar{b}$ is kinematically suppressed. But a $bc\bar{b}$ final state would clearly be swamped by QCD background. Noting that the same argument would hold for the case of finite ρ_{tc} but all other ρ_{ij} 's negligible, we turn to the ILC at 500 GeV.

Our signal process of Eq. (1.1) is electroweak production of the H^+H^- pair. The similar process at LHC with $c\bar{b}c\bar{b}$ final state is clearly swamped by QCD background.

A nonzero ρ_{tc} can drive the same-sign top channel via $H, A \rightarrow t\bar{c}, \bar{t}c$ in the process of Eq. (1.2), where the HA is produced via Z boson only, with ZHA coupling $\propto s_\gamma$ [31]. Although the same-sign top signature would make clear the g2HDM origin, but as argued, having missing energy and mass due to two unseen neutrinos in the final state, m_{H^+} reconstruction is not possible.

Let us not repeat the discussion already given in the Introduction, but just note from Fig. 1 that the two other processes brought in to help salvage mass reconstruction both turn out to have too small cross sections to be relevant. But interestingly, the main process of Eq. (1.1) turns out to actually allow m_{H^+} extraction, which utilizes the kinematics of effective two-body production, as we will show. But let us first go through the signal of Eq. (1.1) and the corresponding background processes.

3 Signal and background processes

For our signal channel of $e^+e^- \rightarrow H^+H^- \rightarrow c\bar{b}c\bar{b}$, we consider a final state of two b -jets plus two light jets.

We use Madgraph [39] to generate the samples for the signal using the 2HDM model formulated via Feynrules [40]. We consider all the interfering contributions from SM with our signal, which includes ZZ, Zh , and we assume unpolarized beams in our study. In addition, we include the single charged Higgs contribution $H^+\bar{c}b$. Nevertheless, as we have discussed, this single H^+ associated production is fairly suppressed, and we do not attempt to extract it. We use PYTHIA6.4 for hadronization and modeling of initial state radiation, as discussed in Ref. [41]. We then pass the sample to Delphes3.5.0 [42] for fast detector

simulation, using the default International Linear Detector (ILD) card [43], as well as the anti- k_T algorithm [44] for jet reconstruction.

Whether interfering or not, we generate events for the following backgrounds: $t\bar{t} \rightarrow b\tilde{j}\tilde{j}b\tilde{j}\tilde{j}$; $W^+W^- \rightarrow 4\tilde{j}$; $Zh, ZZ \rightarrow jjb\bar{b}$. Here j is a light jet and $\tilde{j} = j$ or c . We also include backgrounds from $Z \rightarrow b\bar{b}$ (jj) where a gluon is radiated and splits into jj ($b\bar{b}$), which we denote as $b\bar{b}jj$ (QCD). Here, j could also be a gluon; replacing b by c , we get $c\bar{c}\tilde{j}\tilde{j}$ (QCD) background, where c is mistagged as b where mistag rate depends on the transverse momentum of a c as described in the default ILD card [43].

Tagging of b brings out a special category that we call $b\bar{b}b\bar{b}$, which can be fed by Zg^* , Zh and ZZ , where Zg^* is the aforementioned QCD process but with $jj = b\bar{b}$, where we let b -tagging run its course (a similar effect for $c\bar{c}c\bar{c}$ is absorbed into $c\bar{c}\tilde{j}\tilde{j}$ (QCD)). We follow the same procedure as signal to generate background events.

We choose $m_{H^+} = m_H = m_A = 200$ GeV and set all $\rho_{ij} = 0$, except $\rho_{tc} = \rho_{tt} = 0.1$, with $c_\gamma = 0$. These choices force H^+, A, H to decay only via ρ_{tc} and ρ_{tt} , i.e. $H^+ \rightarrow c\bar{b}, t\bar{b}$ and $H, A \rightarrow t\bar{c}, \bar{t}c$. The decay widths are 0.127, 0.008 and 0.008 GeV, respectively.

To select the events, we require

- $p_T(j, b) > 20$ GeV, $|\eta(j, b)| < 2.5$;
- Number of b -jets and light jets: $N_b = 2, N_j = 2$;
- Number of isolated leptons = 0.

Note that the p_T and η cut are intrinsic cuts of the ILD card. The requirement of no isolated leptons removes most of the $t\bar{t} \rightarrow bj\bar{j}b\ell\nu$ background (labeled as $tt4\tilde{j}$). We denote the above selection requirements as Cuts A.

Process	Cuts A	Cuts B
$c\bar{b}c\bar{b}$ ($H^+H^- + \text{SM}$)	10.2 fb	5.0 fb
$c\bar{c}c\bar{b}$ (SM-only)	4.9 fb	1.7 fb
$t\bar{t}$	15.3 fb	8.3 fb
$b\bar{b}j\tilde{j}$ (QCD)	13.1 fb	9.7 fb
$c\bar{c}\tilde{j}\tilde{j}$ (QCD)	2.7 fb	1.6 fb
$b\bar{b}b\bar{b}$	3.3 fb	1.7 fb
ZZ	6.3 fb	1.0 fb
Zh	7.8 fb	0.4 fb
W^+W^-	2.5 fb	1.7 fb
Total (SM-only)	55.8 fb	26.1 fb
Total ($H^+H^- + \text{SM}$)	61.1 fb	29.5 fb
Significance ($\mathcal{L} = 1 \text{ ab}^{-1}$)	22.1	20.2

Table 1. Cross sections in fb of the interfering Signal and rest of the backgrounds. We also show $c\bar{b}c\bar{b}$ contribution for SM only after Cuts A and Cuts B. See text for more details

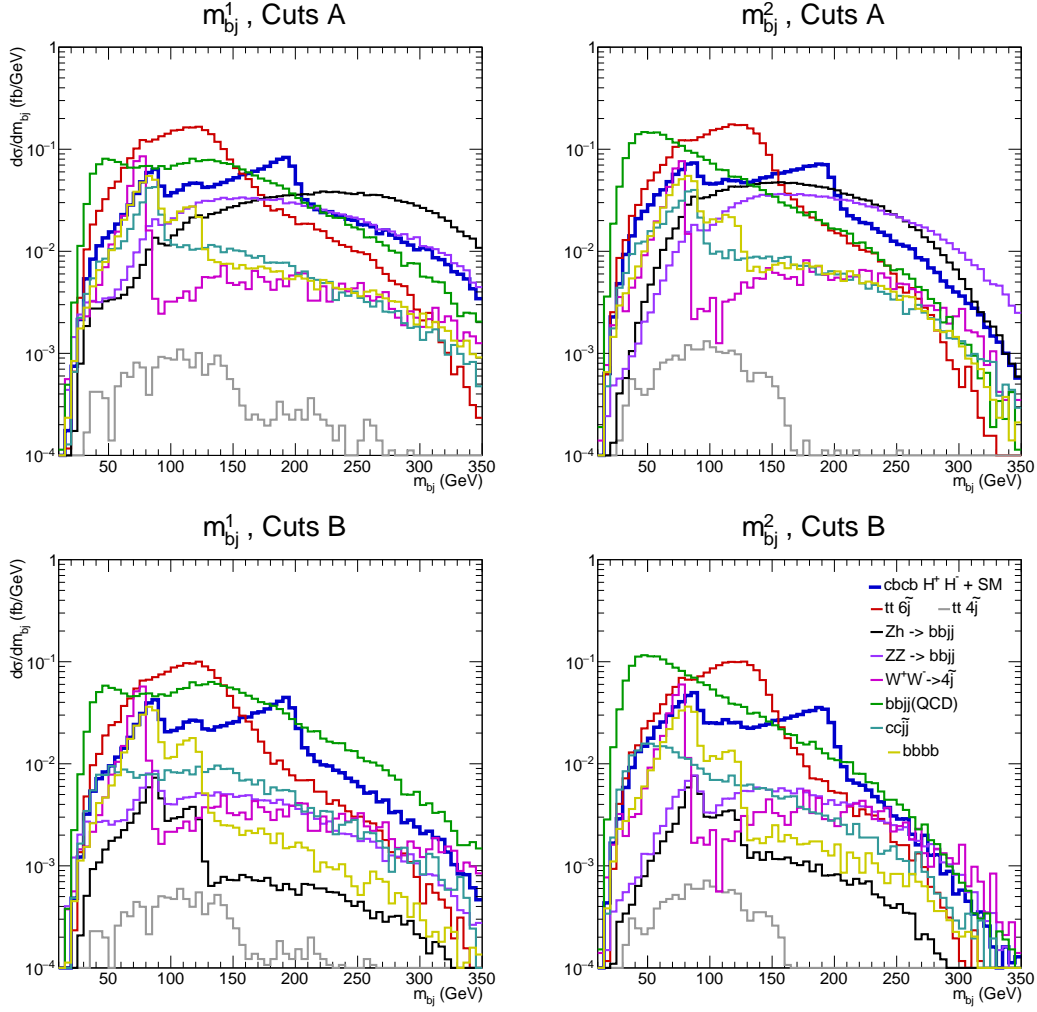


Figure 2. Reconstructed m_{bj} from both bj pairs, following Cuts A and B. See text for more details.

Next, we veto all events that satisfy $|m_{bb}(m_{jj}) - m_Z| < 15$ GeV, $|m_{bb} - m_h| < 20$ GeV to reduce Zh and ZZ backgrounds, where $m_{bb}(m_{jj})$ is the reconstructed mass of two b -tagged (j) jets. We denote this Z, h veto as Cuts B. In Table 1 we present our estimates of the cross sections after applying Cuts A and B. We could apply a cut to veto the events with m_W , but since W^+ and H^+ masses are far apart, we do not gain much in doing so.

In Fig. 2, we show in the top and bottom frames the reconstructed m_{bj} pairs after applying Cuts A and Cuts B. Here we select a b -jet and j which are in closer angular proximity to each other. This separates the two pairs, and gives rise to some mild difference between left and right panels. Our attempt to access the mass of H^+ is discussed in the next section.

We also give our significance estimates in Table 1. Since our signal interferes with SM (at a negligible 2%), we first estimate the SM only contribution to $c\bar{b}c\bar{b}$ final state and combine this with the other non-interfering backgrounds as discussed above. We call this

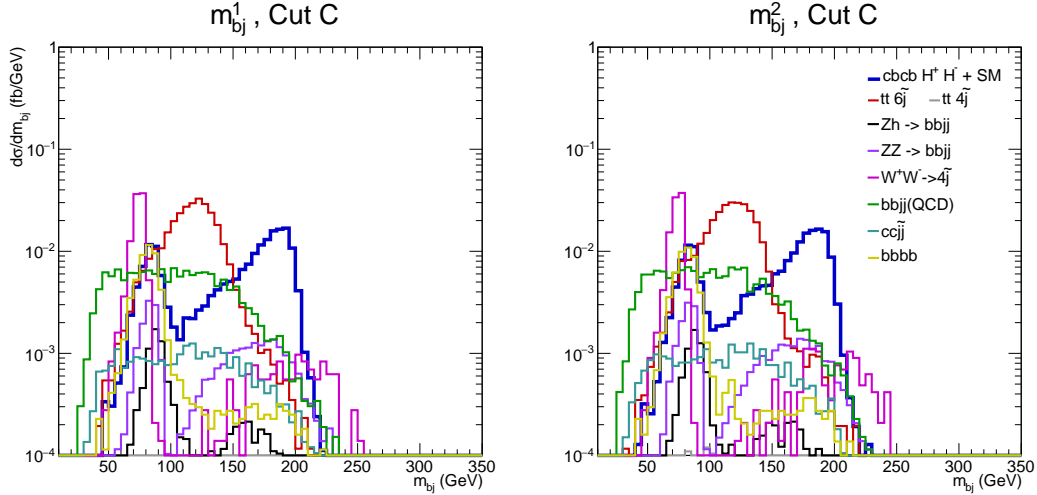


Figure 3. Reconstructed m_{bj} from both bj pairs, following Cut C, Eq. (4.1). See text for more details.

total cross section as the SM-only contribution. We estimate significance with $\mathcal{L} = 1 \text{ ab}^{-1}$. Suppose we have n_{pred} events from SM, while including the H^+H^- contribution we have n events. The significance is then estimated using the likelihood of a simple counting experiment as [45],

$$Z(n|n_{\text{pred}}) = \sqrt{-2 \ln \frac{L(n|n_{\text{pred}})}{L(n|n)}}, \quad (3.1)$$

where $L(n_1|n_0) = e^{-n_1} n_1^{n_0} / n_0!$.

4 Prospects for Discovery and Mass Extraction

In this section we discuss the prospect for discovery of our signal. We see from Table 1 that the H^+H^- signal can enhance the $bbjj$ final state significantly. But to demonstrate we do have $H^+ \rightarrow c\bar{b}$, we attempt at further improvements with mass extraction in mind.

We first tried the scalar sum, H_T , of the strength of p_T of all four jets by requiring $H_T \geq 300 \text{ GeV}$. This improves our significance from $\simeq 21\sigma$ to 22.5σ as compared with Cuts B, but it is not so different from Cuts A. For our second approach, we note that to extract the charged Higgs mass, one needs to identify the correct bottom and charm pairing, to which we turn to discuss.

Towards m_{H^+} Extraction.— The H^+H^- pair turns into four-jets, and one could misidentify the pairing. To identify the correct pairing, we first select one b -tagged jet, and chose from the two light jets the one at closer angular proximity to the selected b -jet. This is not very effective for the 500 GeV ILC. We denote this reconstructed pair mass m_{bj}^1 and the remaining pair as m_{bj}^2 , which is what is plotted in Fig. 2. Note that Delphes orders the jets by p_T , so our choice causes a certain bias that makes the two distributions a little different, as already mentioned. To improve the right pairing, we then apply the condition

$$|m_{bj}^1 - m_{bj}^2| < 0.1 \times m_{bj}^1. \quad (4.1)$$

The 0.1 factor is somewhat arbitrarily chosen for sake of retaining statistics, with no attempt at optimization to make $m_{bj}^1 = m_{bj}^2$ more restrictive. We call the approximate equality condition of Eq. (4.1) Cut C. The distribution of m_{bj}^1 and m_{bj}^2 after applying Cut C is presented in Fig. 3, with cross sections given in Table 2.

“Edge” at m_{H^+} . — Cut C turns out to be very powerful at rejecting background while suitably efficient in retaining our signal. Inspecting the reconstructed $m_{bj}^{1,2}$ distributions reveal a peculiar “Jacobian”-like drop of signal around 200 GeV, analogous to what we see with $W \rightarrow \ell\nu$ transverse mass plot. Note that the cut of Eq. (4.1) itself does not import any mass information.

One may notice that we have kept the $W^+W^- \rightarrow 4\tilde{j}$ background (magenta) and have not vetoed it. This would practically be $c\bar{s}\bar{c}s$ with both charm mistagged as b -jets, as the ILD card of Delphes is able to do. One can see the same behavior of an “edge” around the W mass. This suggest that it is a common effect due to two-body production in the C.M. frame, since at the ILC one collides e^+ and e^- without parton distributions as at hadron colliders. As a result, we have exact knowledge of the kinematics, resulting in maximum possible available transverse momentum for the charged Higgs, approximated by $p_T^{\max}(H^+) = |\vec{p}_{H^+}| = \sqrt{s/4 - m_{H^+}^2}$, which is $\simeq 150$ (458) GeV for 500 GeV (1 TeV) ILC. Beyond this there is barely any event, which creates a Jacobian-like fall after 200 (150) GeV for reconstructed m_{bj} ($p_T^{H^+}$).

In case of pp collider, we expect some spread in distribution due to parton momenta. To confirm this we reconstruct m_{bj} using the same procedure for a pp collider with $\sqrt{s} = 14$ TeV and compare with e^+e^- at $\sqrt{s} = 1$ TeV. The results with arbitrary scale are compared in Fig. 4(a), along with a truth level $p_T^{H^+}$ from both e^+e^- and pp colliders in Fig. 4(b). The $p_T^{H^+}$ at e^+e^- collider drops sharply at ~ 460 GeV, while for the pp collider it is stretched out by parton distributions as the H^+H^- pair is not in the C.M. frame. For the m_{bj} distribution, we see the sharp “edge” at 200 GeV for e^+e^- collider. In comparison, for pp

Process	Cut C	Mass Cut
$c\bar{b}\bar{c}b$ ($H^+H^- + \text{SM}$)	0.99 fb	0.51 fb
$c\bar{b}\bar{c}b$ (SM-only)	0.29 fb	0.02 fb
$t\bar{t}$	1.51 fb	0.03 fb
$b\bar{b}j\bar{j}$ (QCD)	0.77 fb	0.06 fb
$c\bar{c}j\bar{j}$ (QCD)	0.13 fb	0.02 fb
$b\bar{b}b\bar{b}$	0.27 fb	0.01 fb
ZZ	0.15 fb	0.04 fb
Zh	0.04 fb	0.01 fb
W^+W^-	0.55 fb	0.02 fb
Total (SM-only)	3.72 fb	0.21 fb
Total ($H^+H^- + \text{SM}$)	4.42 fb	0.68 fb
Significance ($\mathcal{L} = 1 \text{ ab}^{-1}$)	11.1	26.3

Table 2. Same as Table 1, but after Cut C and Mass Cut. See text for more details.

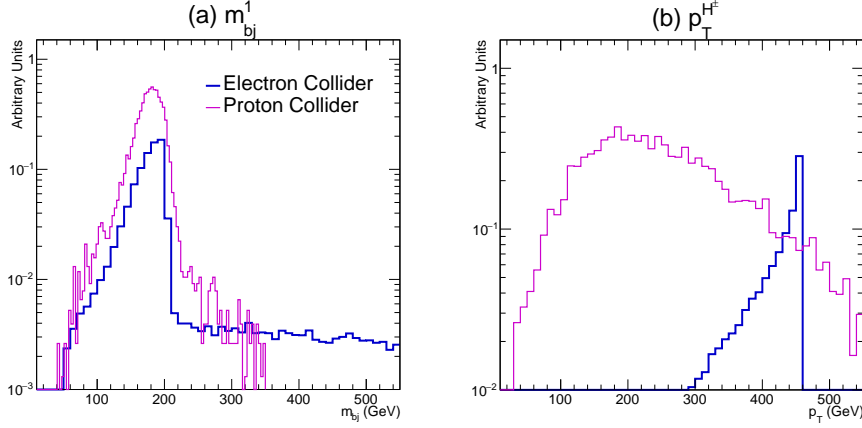


Figure 4. Comparison of (a) reconstructed m_{bj}^1 , and (b) $p_T^{H^\pm}$ at truth level from $e^+e^- \rightarrow H^+H^- \rightarrow c\bar{c}b$ (blue) at $\sqrt{s} = 1$ TeV and $pp \rightarrow H^+H^- \rightarrow c\bar{c}b$ (magenta) at $\sqrt{s} = 14$ TeV after Cuts A.

collider, there is some hint of the “edge”. However, given the leading order cross section after Cuts A is only at 1.2 fb level at 14 TeV, it would be completely swamped by much larger QCD background.

Improvement with C.M. Energy.— The angular proximity requirement described as Cuts A would work better at higher C.M. energy, as the H^\pm boson becomes more boosted. In Fig. 5 we show the reconstructed m_{bj}^1 after Cuts A for $\sqrt{s} = 500$ GeV and 1 TeV. We see clearly that the peak around m_{H^\pm} becomes more prominent for 1 TeV case than for 500 GeV, and the “edge” also appears sharper. Further improvements can be achieved by applying a cut on the charged Higgs transverse momentum, but we do not explore this possibility further.

Following Fig. 3, one can extract m_{H^\pm} from fitting “the edge”, which we leave to future experiments to do. We apply the mass window cut of $160 \text{ GeV} \leq m_{bj} \leq 210 \text{ GeV}$ on both pairs after Cut C, which we call the Mass Cut. The lower value is chosen by comparing with background, which the experimental analysis can do much better. We find that the significance jumps to 26.3σ . The results after Cut C and the Mass Cut are presented in Table 2. While our result shows some scope for mass reconstruction but we have not included systematic uncertainties, uncertainties in the detector resolution etc. in our analysis. We remark that such uncertainties would alleviate the possibility of m_{H^\pm} reconstruction to some extent. We leave out such a detailed analysis for future.

Our focus of interest was a parameter space where all ρ_{ij} s are vanishingly small but ρ_{tc} is nonzero with $m_{H^\pm} \simeq m_H \simeq m_A \simeq 200$ GeV. Such a parameter space renders a blind spot for discovery at the LHC. We now discuss briefly the impact of different ρ_{ij} s on the discovery of Eq. (1.1). Presence of such couplings would alleviate the discovery potential via suppression in the $H^\pm/H^\mp \rightarrow c\bar{c}/\bar{c}b$ branching ratios. In general, $\rho_{ii} \sim \lambda_i$ i.e. $\rho_{tt} \sim \lambda_t$, $\rho_{bb} \sim \lambda_b$ etc. As for example, it has been found that $|\rho_{tt}| \gtrsim 0.4$ is excluded for $m_{H^\pm} \simeq m_H \simeq m_A \simeq 200$ GeV via direct and indirect searches [46, 47]. Therefore the impact of $|\rho_{tt}|$ on discovery would be largest if we saturate the coupling to its upper limit

0.4. As for illustration we plotted in the Fig. 6 the 5σ and 3σ contours for the process in Eq. (1.1) at $\sqrt{s} = 500$ GeV for $m_{H^+} = 200, 220$ GeV and 2σ contour for 240 GeV in the $|\rho_{tt}|$ - $|\rho_{tc}|$ plane. While generating Fig. 6 the selection cuts are kept as in before for $m_{H^+} = 200$ GeV but, for $m_{H^+} = 220$ (240) GeV we changed $180 \text{ GeV} < m_{b_j} < 230$ GeV, ($200 \text{ GeV} < m_{b_j} < 250$ GeV). In finding in Fig. 6 we rescaled the $\sigma \times \mathcal{B}(H^+/H^- \rightarrow c\bar{b}/\bar{c}b)$ of the process in Eq. (1.1) and ignored mild interference effects for simplicity. Further, for both $m_{H^+} = 200$ and 220 GeV we chose integrated luminosity 1 ab^{-1} . However, for 240 GeV due to the rapid fall in the cross section near the threshold of the $\sqrt{s} = 500$ CM energy one may only have 2σ significance with 10 ab^{-1} which is shown by the dashed red contour in the right panel of Fig. 6. It should also be noted that for a fixed value of ρ_{tt} one may need a larger ρ_{tc} for $m_{H^+} = 220$ GeV compared $m_{H^+} = 200$ GeV. This is again simply due to the fall in cross sections as we approach to the $m_{H^+} = \sqrt{s}/2$ threshold. It is clear from the Fig. 6 that if $|\rho_{tt}|$ is large one would require larger $|\rho_{tc}|$ for discovery for all three chosen masses. Note that achievable significance reduces when $|\rho_{tt}|$ becomes large for all three m_{H^+} in Fig. 6. Impact of nonvanishing ρ_{bb} is expected to be mild since it is more stringently constrained than $|\rho_{tt}|$ for our target mass ranges [48]. A discovery of $e^+e^- \rightarrow \gamma^*/Z^* \rightarrow H^+H^- \rightarrow c\bar{b}\bar{c}b$ is possible for m_{H^+} below our target mass range 200 GeV however for $m_{H^+}, m_H, m_A < m_t$ we are subjected to additional constraints arising from different direct and indirect searches. E.g. if $m_A = m_H = m_{H^\pm} \lesssim m_t + m_c(m_b)$ GeV one may have processes such as $pp \rightarrow t\bar{t}$ followed by $t \rightarrow cH/A, t \rightarrow H^\pm b$ decays as potential discovery modes at the LHC. In addition, observables such as $\mathcal{B}(B \rightarrow X_s \gamma)$ and $B_{s,d}$ mixing would provide stringent constraints for ρ_{tc} via charged Higgs-top-charm-quark loop [9]. In our exploratory analysis we have not considered such parameter space and leave out a detailed analysis for future.

5 Discussion and Conclusion

We have given the scenario of relatively weak ρ_{tc} and ρ_{tt} couplings — still sufficient for EWBG for the latter — together with light H, A, H^\pm , degeneracy at ~ 200 GeV, that

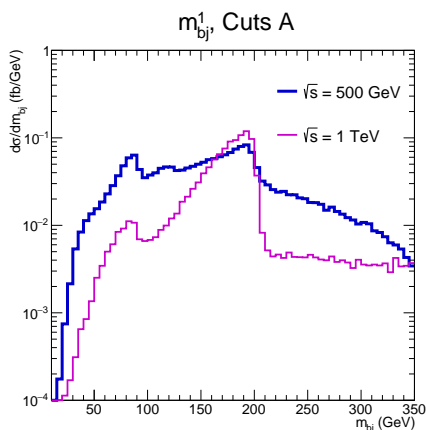


Figure 5. Reconstructed $m_{b_j}^1$ after Cuts A for 500 GeV (blue) and 1 TeV (magenta) C.M. energies.

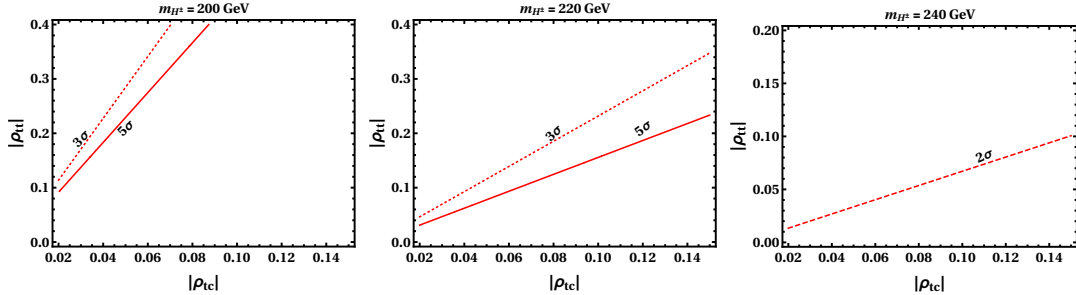


Figure 6. The 5σ and 3σ contours in $\rho_{tt}-\rho_{tc}$ plane of the $e^+e^- \rightarrow \gamma^*/Z^* \rightarrow H^+H^- \rightarrow c\bar{c}b\bar{b}$ process at $\sqrt{s} = 500$ GeV for $m_{H^+} = 200$ (left panel) and 220 GeV (middle panel) respectively. With the same CM energy we also plotted 2σ contour for $m_{H^+} = 240$ GeV in the right panel. Here we assumed 1 ab^{-1} integrated luminosity for $m_{H^+} = 200$ and 220 GeV but 10 ab^{-1} for 240 GeV. See text for details.

could evade LHC search. That is, the $cg \rightarrow tH/tA \rightarrow tt\bar{c}$, $tt\bar{t}$ cross sections become too low, while $cg \rightarrow bH^+$ production ends dominantly in $b\bar{c}b$ final state. But the electroweak production of $e^+e^- \rightarrow \gamma^*/Z^* \rightarrow H^+H^- \rightarrow c\bar{c}b\bar{b}$ not only can be discovered with high significance at the ILC operating at 500 GeV, but provide H^+ mass through this “edge”, or sharp fall of m_{bj} distribution after applying the equal pair mass filter. In the small ρ_{tt} limit, the $c\bar{c}b\bar{b}$ electroweak production through $e^+e^- \rightarrow H^+H^-$ is even independent of the ρ_{tc} strength. But in consideration of electroweak baryogenesis, we have kept $\rho_{tt} \sim \mathcal{O}(0.1)$, which is still robust [1] for generating BAU. Such ρ_{tt} strength can be measured via the kinematically suppressed $t\bar{b}c\bar{b}$ production.

We have elucidated the cause for the “edge” that facilitates the extraction of m_{H^+} as due to the two-body kinematics of H^+H^- pair production in the center of mass frame. For this purpose, we have not vetoed W^+W^- production in Figs. 2 and 3. One clearly sees from Figs. 3 the “edge” at M_W from the $c\bar{s}c\bar{s}$ final state, which can be used as a demonstration mode. Furthermore, $W^+W^- \rightarrow c\bar{s}l\nu$ can be fully reconstructed, and one can clearly separate the two W ’s as further check.

The latter point brings about a comment of curiosity. The muon $g-2$ anomaly has recently been confirmed [49] by the muon $g-2$ collaboration at FNAL. It has been suggested [50] that it could be explained by the one-loop mechanism in g2HDM with sizable $\rho_{\tau\mu} \simeq \rho_{\mu\tau}$, where for $m_{H,A} \sim 200$ GeV, the strength does not need to be as large as 0.2 . On one hand this illustrates the versatility and richness of the phenomenology of g2HDM, while on the other hand one might have the $c\bar{b}\tau\nu$ discovery mode analogous to the $c\bar{s}\tau\nu$ for W^+W^- that we just mentioned. However, the $\rho_{\tau\mu} \simeq \rho_{\mu\tau}$ coupling strength would be larger than our ρ_{tc} , ρ_{tt} values, hence the H , A , H^+ bosons would likely be discovered already at the LHC, as discussed in Ref. [50], and the ILC would be needed less.

We can also have flavor diagonal process like $e^+e^- \rightarrow Z^* \rightarrow HA \rightarrow 4b, 4\tau, 2b2\tau$, but these process require a non-zero ρ_{bb} and $\rho_{\tau\tau}$. In this study we have $\rho_{bb}, \rho_{\tau\tau} \rightarrow 0$ hence these channels are highly suppressed. Interested reader can look at Ref [48] where they have considered $4b$ final state at ILC, in a ρ_{bb} driven EWBG scenario.

In conclusion, if extra top Yukawa couplings turn out weak while the extra H, A, H^+

bosons turn out light, even the HL-LHC may not be able to uncover them. We show, with example of $m_H \sim m_A \sim m_{H^+} \sim 200$ GeV, that the electroweak production of $e^+e^- \rightarrow H^+H^- \rightarrow c\bar{b}c\bar{b}$ may not only reveal the presence of such physics, but allow the extraction of m_{H^+} . The $t\bar{b}c\bar{b}$ mode can provide information on ρ_{tt} and check whether electroweak baryogenesis is achievable. The presence of H and A can be revealed in same-sign top, or $t\bar{t}c$ ($\bar{t}tc$) production, but how to access m_H , m_A needs further study.

Acknowledgments WSH and RJ are supported by MOST 110-2639-M-002-002-ASP of Taiwan, with WSH in addition by NTU 110L104019 and 110L892101. TM is supported by a postdoctoral research fellowship from the Alexander von Humboldt Foundation.

References

- [1] K. Fuyuto, W.-S. Hou and E. Senaha, Phys. Lett. B **776**, 402 (2018) [arXiv:1705.05034 [hep-ph]].
- [2] C.-Y. Chen, H.-L. Li and M. Ramsey-Musolf, Phys. Rev. D **97**, 015020 (2018) [arXiv:1708.00435 [hep-ph]].
- [3] S.L. Glashow and S. Weinberg, Phys. Rev. D **15**, 1958 (1977).
- [4] K. Fuyuto, W.-S. Hou and E. Senaha, Phys. Rev. D **101**, 011901 (2020) [arXiv:1910.12404 [hep-ph]].
- [5] M. Kohda, T. Modak and W.-S. Hou, Phys. Lett. B **776**, 379 (2018) [arXiv:1710.07260 [hep-ph]].
- [6] W.-S. Hou, M. Kohda and T. Modak, Phys. Lett. B **786**, 212 (2018) [arXiv:1808.00333 [hep-ph]].
- [7] W.-S. Hou, M. Kohda and T. Modak, Phys. Lett. B **798**, 134953 (2019) [arXiv:1906.09703 [hep-ph]].
- [8] A.M. Sirunyan *et al.* [CMS], Eur. Phys. J. C **78**, 140 (2018) [arXiv:1710.10614 [hep-ex]].
- [9] B. Altunkaynak, W.-S. Hou, C. Kao, M. Kohda and B. McCoy, Phys. Lett. B **751**, 135 (2015) [arXiv:1506.00651 [hep-ph]].
- [10] G. Aad *et al.* [ATLAS], Phys. Lett. B **716**, 1 (2012) [arXiv:1207.7214 [hep-ex]].
- [11] S. Chatrchyan *et al.* [CMS], Phys. Lett. B **716**, 30 (2012) [arXiv:1207.7235 [hep-ex]].
- [12] W.-S. Hou and M. Kikuchi, EPL **123**, 11001 (2018) [arXiv:1706.07694 [hep-ph]].
- [13] W.-S. Hou and T. Modak, Mod. Phys. Lett. A **36**, 2130006 (2021) [arXiv:2012.05735 [hep-ph]].
- [14] W.-S. Hou and G. Kumar, Phys. Rev. D **102**, 115017 (2020) [arXiv:2008.08469 [hep-ph]].
- [15] A.M. Sirunyan *et al.* [CMS], JHEP **09**, 007 (2018) [arXiv:1803.06553 [hep-ex]].
- [16] G. Aad *et al.* [ATLAS], Phys. Rev. Lett. **125**, 051801 (2020) [arXiv:2002.12223 [hep-ex]].
- [17] A.M. Sirunyan *et al.* [CMS], JHEP **03**, 103 (2020) [arXiv:1911.10267 [hep-ex]].
- [18] A.M. Sirunyan *et al.* [CMS], JHEP **08**, 113 (2018) [arXiv:1805.12191 [hep-ex]].
- [19] G. Aad *et al.* [ATLAS], Phys. Rev. D **102**, 032004 (2020) [arXiv:1907.02749 [hep-ex]].

- [20] M. Aaboud *et al.* [ATLAS], Phys. Rev. Lett. **119**, 191803 (2017) [arXiv:1707.06025 [hep-ex]].
- [21] A.M. Sirunyan *et al.* [CMS], JHEP **04**, 171 (2020) [arXiv:1908.01115 [hep-ex]].
- [22] A.M. Sirunyan *et al.* [CMS], JHEP **07**, 126 (2020) [arXiv:2001.07763 [hep-ex]].
- [23] G. Aad *et al.* [ATLAS], JHEP **06**, 145 (2021) [arXiv:2102.10076 [hep-ex]].
- [24] G. Aad *et al.* [ATLAS], Eur. Phys. J. C **73**, 2465 (2013) [arXiv:1302.3694 [hep-ex]].
- [25] A.M. Sirunyan *et al.* [CMS], Phys. Rev. D **102**, 072001 (2020) [arXiv:2005.08900 [hep-ex]].
- [26] M. Aaboud *et al.* [ATLAS], JHEP **09**, 139 (2018) [arXiv:1807.07915 [hep-ex]].
- [27] A.M. Sirunyan *et al.* [CMS], JHEP **07**, 142 (2019) [arXiv:1903.04560 [hep-ex]].
- [28] A.G. Akeroyd and W.J. Stirling, Nucl. Phys. B **447**, 3 (1995).
- [29] A.G. Akeroyd, S. Moretti and M. Song, Phys. Rev. D **98**, 115024 (2018) [arXiv:1810.05403 [hep-ph]].
- [30] A.G. Akeroyd, S. Moretti and M. Song, Phys. Rev. D **101**, 035021 (2020) [arXiv:1908.00826 [hep-ph]].
- [31] W.-S. Hou and G.-L. Lin, Phys. Lett. B **379**, 261 (1996) [arXiv:hep-ph/9510359 [hep-ph]].
- [32] S. Davidson and H. E. Haber, Phys. Rev. D **72**, 035004 (2005) [erratum: Phys. Rev. D **72**, 099902 (2005)] [arXiv:hep-ph/0504050 [hep-ph]].
- [33] K.-F. Chen, W.-S. Hou, C. Kao and M. Kohda, Phys. Lett. B **725**, 378 (2013) [arXiv:1304.8037 [hep-ph]].
- [34] G.C. Branco, P.M. Ferreira, L. Lavoura, M.N. Rebelo, M. Sher and J.P. Silva, Phys. Rept. **516**, 1 (2012) [arXiv:1106.0034 [hep-ph]].
- [35] D.K. Ghosh, W.-S. Hou and T. Modak, Phys. Rev. Lett. **125**, 221801 (2020) [arXiv:1912.10613 [hep-ph]].
- [36] W.-S. Hou, M. Kohda, T. Modak and G.-G. Wong, Phys. Lett. B **800**, 135105 (2020) [arXiv:1903.03016 [hep-ph]].
- [37] A.M. Sirunyan *et al.* [CMS], Eur. Phys. J. C **79**, 421 (2019) [arXiv:1809.10733 [hep-ex]].
- [38] G. Aad *et al.* [ATLAS], Phys. Rev. D **101**, 012002 (2020) [arXiv:1909.02845 [hep-ex]].
- [39] J. Alwall, M. Herquet, F. Maltoni, O. Mattelaer and T. Stelzer, JHEP **06**, 128 (2011) [arXiv:1106.0522 [hep-ph]].
- [40] A. Alloul, N.D. Christensen, C. Degrande, C. Duhr and B. Fuks, Comput. Phys. Commun. **185**, 2250 (2014) [arXiv:1310.1921 [hep-ph]].
- [41] T. Sjöstrand, S. Mrenna and P.Z. Skands, JHEP **05**, 026 (2006) [arXiv:hep-ph/0603175 [hep-ph]].
- [42] J. de Favereau *et al.* [DELPHES 3], JHEP **02**, 057 (2014) [arXiv:1307.6346 [hep-ex]].
- [43] T. Behnke *et al.*, [arXiv:1306.6329 [physics.ins-det]].
- [44] M. Cacciari, G.P. Salam and G. Soyez, JHEP **04**, 063 (2008) [arXiv:0802.1189 [hep-ph]].
- [45] G. Cowan, K. Cranmer, E. Gross and O. Vitells, Eur. Phys. J. C **71**, 1554 (2011) [erratum: Eur. Phys. J. C **73**, 2501 (2013)] [arXiv:1007.1727 [physics.data-an]].
- [46] S.M. Lee, T. Modak, K.-y. Oda and T. Takahashi, Eur. Phys. J. C **82**, 18 (2022) [arXiv:2108.02383 [hep-ph]].

- [47] T. Modak and K.-y. Oda, Eur. Phys. J. C **80**, 863 (2020) [arXiv:2007.08141 [hep-ph]].
- [48] T. Modak and E. Senaha, Phys. Lett. B **822**, 136695 (2021) [arXiv:2107.12789 [hep-ph]].
- [49] B. Abi *et al.* [Muon g-2], Phys. Rev. Lett. **126**, 141801 (2021) [arXiv:2104.03281 [hep-ex]].
- [50] W.-S. Hou, R. Jain, C. Kao, G. Kumar and T. Modak, Phys. Rev. D **104**, 075036 (2021) [arXiv:2105.11315 [hep-ph]].